International Journal of Environmental Science and Technology (2022) 19:9095–9106
https://doi.org/10.1007/s13762-021-03773-6

ORIGINAL PAPER

Impacts of sodium bicarbonate and co-amine monomers on properties of thin-film composite membrane for water treatment

J. O. Origomisan[1,2,3,4] · W. J. Lau[1,2] · F. Aziz[1,2] · A. F. Ismail[1,2] · A. Adewuyi[3,4] · Y. O. Raji[1,2] · S. O. Lai[5]

Received: 15 April 2021 / Revised: 31 July 2021 / Accepted: 30 October 2021 / Published online: 15 November 2021

Abstract

Polyamide (PA) thin-film composite (TFC) nanofiltration (NF) membranes are widely used for the treatment of water and wastewater treatment. However, the membrane surface properties could be further modified during interfacial polymerization (IP) process to achieve higher water flux and salt rejection. Herein, the effects of sodium bicarbonate ($NaHCO_3$) and co-amine monomer—2-(2′aminoethoxy) ethylamine (AEE) on the characteristics of piperazine (PIP)-based TFC membranes were investigated for water purification and aerobically treated palm oil mill effluent (AT-POME) treatment. Characterizations based on field emission scanning electron microscopy (FESEM), Fourier transform infrared analysis (FTIR) and contact angle were carried out to provide support to the filtration results. Our findings showed that 0.5 wt% $NaHCO_3$ was the best loading to be added to improve the membrane performance by enhancing water permeability by 37% without affecting Na_2SO_4 rejection. In the presence of 0.5 wt% $NaHCO_3$, it is found that the introduction of AEE into PIP solution could further improve the Na_2SO_4 rejection of PIP-based membrane from 97.1 to 98.5% while producing a permeate of better quality. Further evaluation using AT-POME indicated that the AEE-modified membrane was able to enhance the separation performance of PIP-based membrane, increasing its conductivity, colour (ADMI) and COD reduction from 74.31, 92.79 and 83.4%, respectively, to 79.15, 94.26 and 89.3%. This work demonstrated the positive features of using inorganic additive and secondary amine monomer in improving characteristics of TFC membrane for water and wastewater treatment.

Keywords Thin-film composite membrane · Monomer · Salt rejection · Polyamide · Nanofiltration · AT-POME · Antifouling

Introduction

The use of membrane-based separation in treating water and wastewater has been a technology that is easy to scale up and energy-efficient. And amongst different types of membrane structures, polyamide (PA) thin-film composite (TFC) membrane made by the concept of interfacial polymerization (IP) has become the fastest-growing membrane technology for the water purification and industrial wastewater treatment (Lau et al. 2012, Misdan et al., 2013 l Shafiq et al. 2018, Seah et al., 2020) as its selective layer and substrate properties can be easily optimized to achieve the desired separation performance (Xie et al. 2017). Over the years, TFC membranes have experienced tremendous development and application for the markets of nanofiltration (NF) and reverse osmosis (RO) processes (Jiang et al. 2019). The advanced filtration properties of TFC membranes are mainly attributed to its extremely thin layer of highly cross-linked PA layer that acts as a barrier to retain dissolved ions while allowing water molecules to pass through at a faster rate (Huang et al. 2020).

Editorial responsibility: Rangabhashiyam S.

✉ W. J. Lau
lwoeijye@utm.my

1 Advanced Membrane Technology Research Centre (AMTEC), Universiti Teknologi Malaysia, 81310 Skudai, Johor, Malaysia

2 School of Chemical and Energy Engineering, Universiti Teknologi Malaysia, 81310 Skudai, Johor, Malaysia

3 Department of Chemical Sciences, Faculty of Chemical Sciences, Redeemer's University, P.M.B 230, Ede, Osun State, Nigeria

4 African Centre of Excellence for Water and Environmental Research (ACEWATER), Redeemer's University, PMB 230, Ede 232101, Osun State, Nigeria

5 Department of Chemical Engineering, Universiti Tunku Abdul Rahman (UTAR), Sungai Long Campus, Jalan Sungai Long, Bandar Sungai Long, Cheras 43000, Kajang, Selangor, Malaysia

Extensive investigations on the application of TFC NF membranes to produce very freshwater have been carried out in many studies (Chen et al. 2016; Pan et al. 2017; Chong et al. 2019). These kinds of membrane possess the capacity to efficiently remove very small organic compounds, inorganic dissolved ions and molecular contaminants with the size ranging from 200 to 1000 g/mol from water sources. For instance, TFC NF membranes are used in the industries for treatment of textile wastewater via the removal of dyes and ions to reclaim the water. Liu et al. (2017) on the other hand employed self-fabricated TFC NF membranes to achieve 98% chemical oxygen demand (COD) reduction and 74–95% salt rejection during textile wastewater treatment. Another major application of TFC NF membranes is to pre-treat the brackish water and seawater prior to the RO desalination process. The PA layer of these NF membranes provides several advantages including high water flux, unsurpassed salt rejection and excellent chemical resistance. The thick, microporous PSF support layer offers necessary porosity and strength properties under pressure-driven filtration. Unlike the TFC RO membranes that show excellent rejection against monovalent ions (97–99%), the TFC NF membranes are rather unique as they exhibit high divalent ions removal rate but partial separation of monovalent ions (20–80%) (Mollahosseini et al. 2019).

Typically, the performance of TFC membranes could be improved by varying the properties of monomer solution through addition of inorganic salts or introduction of secondary monomers. For instance, Shen et al. (2020) introduced sodium chloride (NaCl) (from range zero to 25 wt%) into the aqueous solution to tune the PA structure of TFC membrane and reported that the water flux and salt rejection of the resultant membrane were improved simultaneously owing to the formation of ultrathin and loose PA layer as a result of decreased mass transfer of amine monomers. Wu et al. (2016) reported that the addition of dimethyl sulfoxide (DMSO) and glycerol in the aqueous phase led to increase in membranes surface hydrophilicity and roughness, producing a TFC membrane with a higher flux without compromising salt rejection. The increased miscibility between aqueous and organic phases by DMSO is the main reason leading to improved membrane structure. In another study, Hao et al. (2019) used calcium chloride ($CaCl_2$) as an additive to enhance PA layer of TFC membrane which led to the increase in rejection and foulant repulsion. This is because calcium ions tend to consume free carboxyl acid groups during the IP process, resulting in the increase in charge repulsion effect therefore reducing membrane fouling.

Sodium bicarbonate ($NaHCO_3$) has also been proved as a promising functional effective additive in optimizing TFC membranes. According to Sun et al. (2018), the presence of $NaHCO_3$ additive during IP process could produce the membrane with significant flux improvement. However, a minor drawback of its addition is that the membrane experienced a slight decline in salt rejection because of the formation of little fissures on the membrane surface. Despite its possibility to enhance membrane water permeation properties, its effect of introducing it into a co-amine monomer mixture during IP process has not been explored. In view of this, $NaHCO_3$ would be used for optimizing the performance of fabricated TFC membranes in this work.

Another emerging method recently being used for the synthesis of PA layer is by applying a co-amine monomer for the fabrication of TFC membranes. The influence of co-amine monomers in aqueous phase is significant as studies have revealed that they play a role in enhancing performances of TFC membranes with respect to flux, solute rejection and antifouling resistances against abiotic and biotic material. Rezania et al. (2019) synthesized a TFC NF membrane by crosslinking a carboxylated aromatic diamine-diol (CDADO) monomer with TMC. The results showed that CDADO exhibited a synergetic effect with PIP and hereby improving membrane hydrophilicity. In respect to salt separation evaluated at 10 bar, the membrane made of CDADO/PIP demonstrated better Na_2SO_4 rejection (~97%) and flux (50 $L/m^2.h$) compared to the regular membrane made of PIP, i.e., 89% rejection and 30 $L/m^2.h$ flux. Improved permeability of membrane made by the mixed amine monomers is attributed to the increased membrane hydrophilicity and smoothness of PA layer which made foulants easily striped away compared to regular PIP-based membrane.

Most recently, several diamine monomers have proved to be very suitable for IP in improving filtration characteristics of TFC NF membranes. 2-(2′Aminoethoxy) ethylamine (AEE)—a diamine monomer possessing an ethyloxy group, which is more hydrophilic and flexible than hydrocarbon diamines is considered in this work as a co-amine monomer. Unlike PEG derivatives with long chains, the swelling of AEE is negligible due to its short molecular chain. The influences of mixed monomers in the aqueous phase are somehow important during membrane fabrication as studies revealed that the existence of secondary monomers could play a role in enhancing performances of TFC membranes (Origomisan et al. 2021).

So far, there has not been enough research effort concentrating on how both an inorganic salt (additive) and a co-amine monomer influence the morphology and filtration performance of the PA layer of TFC membrane for water treatment. Thus, this work aims to investigate the effects of a co-amine monomer (AEE) in the presence of $NaHCO_3$ during IP process on the properties of the PIP/TMC-based NF membrane for enhanced water and wastewater treatment. Asides demonstrating great potential roles in improving the membrane salt rejection and antifouling properties, the separation performance of modified membrane would also be tested with industrial effluent and compared with typical PIP-based membranes.

Materials and methods

Materials

In this work, a commercial polysulfone (PS) substrate (molecular weight cut-off: 20,000 Da) reinforced with nonwoven polyester fabric purchased from the Rising Sun Membrane Technology (Beijing) Co. Ltd (Beijing, China) was used as a support for the fabrication of TFC membranes. The thickness of the substrate together with fabric was approximately 0.159 mm. 2-(2'-aminoethoxy) ethylamine (2,2′-AEE) with molecular weight (MW) of 104.15 g/mol from Sigma-Aldrich together with piperazine (PIP, MW: 86.14 g/mol) and 1,3,5-benzenetricarboxylic acid chloride (TMC, MW: 265.48 g/mol) obtained from Acros Organic were utilized to develop the PA selective layer. Sodium bicarbonate ($NaHCO_3$, MW: 84 g/mol) from Sigma-Aldrich was used as an inorganic additive in the aqueous solution to alter the properties of PA layer formed. Milli-Q RO water (ASTM type III) and n-hexane (Sigma-Aldrich) were used to dissolve 2,2′-AEE/PIP and TMC, respectively, for the preparation of aqueous and organic monomers solution. Sodium sulfate (Na_2SO_4, MW: 142.04 g/mol, Wako Chemicals) was used as charged solute to evaluate the separation performance of fabricated TFC membranes. For antifouling performance evaluation, *bovine serum albumin* (*BSA,* MW: 66,430 g/mol) from Sigma-Aldrich was used as organic foulants to determine the change in water flux against time. All feed solutions for the composite membrane performance evaluation were prepared by dissolving specific quantity of solutes in Milli-Q RO water. The wastewater sample—aerobically treated palm oil mill effluent (AT-POME), was collected from PPNJ Palm Oil Mill Kahang, Johor, Malaysia, and stored at room temperature prior to use.

Preparation of TFC membranes

The PA active layer of TFC membranes was fabricated via the conventional IP technique. Prior to the IP process, the commercial PS substrate in dimension of 11 × 12 cm was soaked for a day in RO in order to eliminate glycerin. Glycerin was applied on the surface of commercial substrate by the manufacturer to keep it wet all the time. A commercial plate roller bought from Sigma-Aldrich was used to drain off excess water on the surface of a substrate after being soaked for 24 h. After the substrate was rolled dry, a rubber gasket followed by an acrylic plate was stacked on top of substrate and the position was strengthened further using stainless steel binder clips. To initiate the IP process, 40 mL of aqueous solution containing 2 wt/v% PIP and different $NaHCO_3$ loading (0, 0.5, 1.5, 2.5 and 3.5 wt%) was initially cast on a horizontal frame. The mixture was then allowed to diffuse through the pores of the substrate for 3 min. Afterwards, the excess solution was removed from the substrate surface followed by dismantling the frame setup. The top surface of the PIP-impregnated substrate was then rolled dry before placing the rubber gasket, acrylic plate, and binder clips back to the substrate. Thereafter, 20 mL of 0.2 wt/v% of TMC in n-hexane was poured into the frame to react with amine monomers. After 1-min reaction time, the TMC in the organic solution was drained off. Following this, the TFC membrane was cured at 60 °C in an electric oven (Model: 101-0BE, XH Home Tool Equipment Factory, China) for 5 min to further enhance the compactness of the PA selective layer before being stored in RO water. Fabrication process of TFC membranes with different co-amine monomer follows the same procedure as stated above with the exception of aqueous solution containing different weight ratio of PIP:AEE (2:0, 1.75:0.25, 1.5:0.5, 1.0:1.0 and 0:2) in the presence of fixed $NaHCO_3$ amount.

Characterization of TFC membranes

The self-synthesized TFC membranes made of different synthesis conditions were characterized and compared in terms of chemical properties and structural morphology. Prior to any characterization, all the fabricated membranes (in size of 2 × 2 cm) were dried in a desiccator for a minimum duration of 24 h. Characterization of chemical structures of membranes was done through Fourier transform Infrared (FTIR) spectrometer (Nicolet 5700, Thermo Scientific) rigged with horizontal and total reflectance accessories. A background analysis was performed prior to each membrane characterization. Spectra of membrane sample were then accumulated from wavenumber ranging from 500 to 4000 cm^{-1} and using resolution of 4 cm^{-1} for the analysis of various functional groups present in each fabricated membrane. Surface and cross-section morphology of fabricated membranes were analysed using field emission scanning electron microscope (FESEM, SU8020, Hitachi) under the magnification ranging from 500× to 30,000×. For surface morphology scanning, the membrane was cut into small piece of about 0.5 cm square and attached on a sample stub using carbon tape. For cross-sectional scanning, the sample was initially freeze-broken in liquid nitrogen for 3 min after which it was sprayed with gold particles prior to FESEM characterization to avoid electrical charge during analysis. The wettability of composite membrane surface was measured by conducting static contact angle measurement using contact angle goniometer (OCA 15Pro, DataPhysics Instruments) based on the sessile drop method. A stainless steel micro-syringe was used to place a drop of RO water (0.5 µL) directly on the skin layer of the fabricated membranes. Drop shape software analysis was then used in achieving the tangent lines of both sides of the membrane. At least 10 measurements were carried out on the surface of same membrane samples to yield the average value.

Water flux and salt rejection determination

The NF performance of fabricated TFC membranes was investigated using a dead-end filtration cell (HP4750, Sterlitech Corp) with a membrane surface area of 14.60 cm^2. The operating pressure employed for the filtration was supplied by high-pressure nitrogen cylinder which was regulated by 2-stage pressure regulator. A membrane coupon with diameter of 5 cm was required for each set of experiment. The dead-end filtration cell was placed on a magnetic stir plate and the stirring speed was maintained at 350 rpm throughout the experiment to determine water flux and rejection. Prior to the filtration process, all the fabricated membranes were compacted using pure water at 15 bar for 30 min until a steady flux was accomplished. Afterwards, the pressure was reduced to 10 bar and the membrane performance was studied. Equations (1) and (2) were used for calculating the pure water flux, W_f (L/m^2.h) and water permeability, A (L/m^2.h.bar) of a membrane, respectively.

$$\mathrm{Wf} = \frac{\mathrm{V}}{\mathrm{A\,T}} \tag{1}$$

$$\mathrm{J} = \frac{W_f}{(\mathrm{P})} \tag{2}$$

where V is total volume of permeate (L), A is effective area of membrane (m^2), T corresponds to the duration taken for filtration (h) and P is the operating pressure (bar). For every single experiment, permeate collected was used to calculate the water flux and water permeability. To get an accurate result, the experiment of same type of membrane was repeated at least three times to yield average value.

The separation performance of the membranes was evaluated at 10 bar using Na_2SO_4 feed solution with concentration of 1000 ppm. The solution was prepared by dissolving 1 g Na_2SO_4 in 1000 mL RO water. Using an electric conductivity meter (Jenway, model 4250), salt concentration of water samples was measured both from the feed and permeate. By applying Eq. (3), salt rejection (R, %) for the fabricated TFC membranes could be calculated.

$$\mathrm{R} = \left(1 - \frac{C_p}{C_f}\right)100 \tag{3}$$

where C_p is total permeate concentration and C_f is total feed solution concentration. Meanwhile, the membrane salt passage was also determined using the same approach and could be determined using Eq. (4). Each TFC membrane was tested at least thrice using different membrane coupons and the average reading was recorded.

$$\text{Salt passage} = \left(\frac{C_p}{C_f}\right)100 \tag{4}$$

The antifouling test was conducted using a new membrane coupon. Prior to the test, each membrane coupon was pre-compacted at 15 bar with pure water. After that, the pure water was replaced with 300-mL NaAlg solution (500 ppm). The membrane performance was then accessed at room temperature at 10 bar. The feed solution was prepared by dissolving 0.5 g NaAlg in 1000 mL RO water. The performance of membrane was examined by observing the change in water flux as a function of filtration time. The water permeability of the membranes (J) was measured every 15 min for a duration of 2 h and the normalized flux (W_f/J) was plotted against time and compared with the initial water flux (W_{f1}) to study the membrane antifouling properties. After completing the test, the fouled membranes were then thoroughly rinsed with RO water for 10 min before continuing to evaluate its flux recovery ability. The obtained pure water flux (W_{f2}) of the rinsed membranes was compared with its initial pure water flux (W_{f1}). The flux recovery rate (FRR, %) of the membranes could then be determined using the following equation:

$$\mathrm{FRR} = \frac{W_{f2}}{W_{f1}}100 \tag{5}$$

Membranes for AT-POME treatment

The separation performances of TFC membranes with respect to water flux as well as key solute/ion rejection for AT-POME were tested following the same procedure as stated in Sect. 2.4. The removal (%) of membranes against conductivity, colour and total organic carbon (TOC) was, respectively, calculated using the following equations.

$$\text{Conductivity removal} = \left(1 - \frac{C_p}{C_f}\right)100 \tag{6}$$

$$\text{Colour removal} = \left(1 - \frac{ABS_p}{ABS_f}\right)100 \tag{7}$$

$$\text{TOC removal} = \left(1 - \frac{TOC_p}{TOC_f}\right)100 \tag{8}$$

where C_p and C_f are ion concentration (mg/L) of feed and permeate, respectively; ABS_p and ABS_f are colour value (abs) of feed and permeate, respectively, and TOC_p and TOC_f are TOC value (mg/L) of feed and permeate, respectively. The conductivity and colour of the water samples were measured using a benchtop conductivity meter (4520, Jenway) and UV–vis spectrophotometer (DR5000, Hach), respectively. Meanwhile, TOC analyser (TOC-LCPN, Shimadzu) was used to determine the level of TOC in the feed and treated water samples. The TOC value of each sample was calculated by subtracting the

total carbon (TC) value obtained with the inorganic carbon (IC) value.

Results and discussion

Impacts of $NaHCO_3$ additive

Surface chemistry and hydrophilicity of membranes

Figure 1a presents the water contact angle of membranes with different $NaHCO_3$ loading ranging from 0 to 3.5 wt% in the aqueous solution. It could be seen that the water contact angle of membranes decreased from 37.48° which is the typical value for the PIP/TMC membrane to 23.15° with increasing $NaHCO_3$ loading. The low contact angle of PIP/TMC membrane (without additive) is due to the specific functional groups of PA layer which contains amide linkage, amine end groups and carboxylic acid end groups (Kazemi et al. 2020). The reduced membrane surface contact angle was attributed to the improved surface hydrophilicity of PA layer upon addition of $NaHCO_3$ and/or changes of the surface roughness based on the Wenzel model. Sun et al. (2018) previously reported the increase in hydrophilic carboxylic groups of PA layer as a result of increasing $NaHCO_3$ loading, leading to the decrease of water contact angle. Further characterization to correlate the change in membrane surface roughness with its contact angle will be provided in the following section.

ATR-FTIR spectra of self-synthesized TFC membranes are presented in Fig. 1b. Overall, there is no great difference in the spectra of all membranes, indicating that the incorporation of small quantity of inorganic additive did not significantly alter the dominant functional groups of the organic PA layer. Another possible reason as to why there was no difference on the membrane surface chemistry can be due the absence of $NaHCO_3$ in the PA matrix as inorganic salt tends to dissolve well in aqueous solution and leach out from the PA layer during IP process. Similar findings were also reported by Fan et al. (2014) and Li et al. (2015) in which the addition of calcium chloride and triethylamine, respectively, into the PA selective layer did not change the FTIR spectra of the resultant TFC membranes. The presence of peaks at 1240 cm^{-1} (asymmetric C–O–C stretching) and 1491 cm^{-1} (CH_3-C-CH_3 stretching) is the typical characteristic peaks of PSf-based substrate. Apart from these, the peaks detected at 1580 cm^{-1} (C-N stretching), 1623 cm^{-1} (C=O stretching of amide group) and 3393 cm^{-1} (O–H stretching of carboxylic acid) indicated the successful formation of the PA layer. To sum up, the addition of $NaHCO_3$ did not change the PA surface chemistry based on the FTIR spectra shown.

TFC membrane performance

The filtration performance of membranes with respect to solute permeability and salt rejection are presented in Fig. 2. It

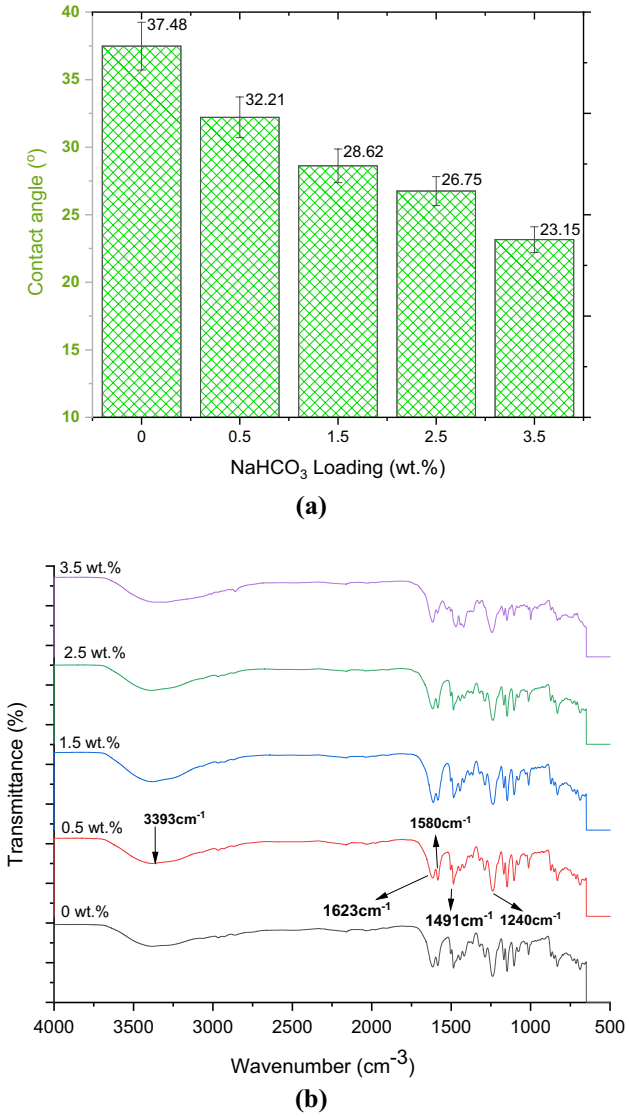

Fig. 1 Impact of $NaHCO_3$ loading on the TFC membrane surface properties, **a** water contact angle and **b** FTIR spectra

was observed that as $NaHCO_3$ additive increased from 0.5 to 2.5 wt%, the membrane water flux was slightly increased from 2.66 to 2.73 L/m^2.h.bar while the Na_2SO_4 rejection was dropped from 97.1 to 94.7%. Compared to the membrane with 2.5 wt% $NaHCO_3$, a significant performance change was observed for the membrane with 3.5wt% $NaHCO_3$ as the membrane water flux was almost doubled up to 4.1 L/m^2.h.bar with a continuous drop in $NaSO_4$ rejection (93.4%). The variation in performance can be explained by the fact that excessive use of $NaHCO_3$ could disturb the cross-link degree of PA, leading to the formation of looser selective layer with enlarged pore size. The increase in $NaHCO_3$ loading could lead to reaction with HCl—a by-product of polymerization reaction between PIP and TMC, forming a PA layer with more hydrophilic carboxylic groups (as evidenced from reduced contact angle). This, as a consequence, produced a lower PA cross-linking degree with higher flux but

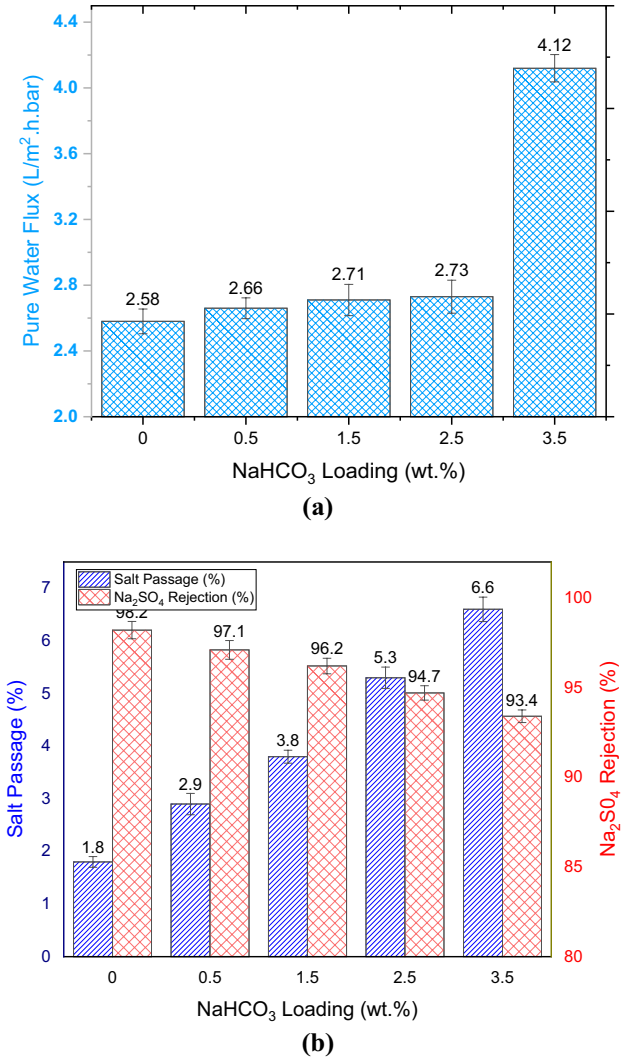

Fig. 2 Effect of $NaHCO_3$ loading on TFC membrane performance with respect to **a** pure water flux and **b** salt passage and Na_2SO_4 rejection

lower rejection rate. Shen et al. (2020) recently reported that the introduction of NaCl into the aqueous phase as an additive could increase membrane pure water flux by ~ 2.5 times in comparison with the control membrane without NaCl.

Compared to the control TFC membrane, it is found that the addition of 0.5 wt% $NaHCO_3$ is the best loading as it could produce the TFC membrane with improved water flux and high degree of hydrophilicity which are important when the membrane is aimed for wastewater treatment. Although the rejection of this modified TFC membrane is slightly lower compared to the control TFC membrane, its rejection rate of 97.1% is still considered acceptable and appropriate for the membranes that will be used for AT-POME treatment. AT-POME sample contains dye pigments that can be easily rejected by NF membrane compared to the dissolved ions. In view of this, 0.5 wt% $NaHCO_3$ was chosen in the following study to study the impacts of co-amine monomer on the TFC membrane properties.

Impacts of a co-amine monomer

Surface chemistry and hydrophilicity of membranes

The surface chemistry composition of self-synthesized membranes made of different PIP:AEE weight ratio in the presence of 0.5 wt% $NaHCO_3$ was analysed by FTIR (Fig. 3a). The presence of peaks at 1149 cm^{-1} (asymmetric C–O–C stretching) and 1488 cm^{-1} (CH_3-C-CH_3 stretching) is the typical characteristic peaks of PSf-based substrate. Adsorption peak at 1149 cm^{-1} is ascribed to C–O–C of AEE monomer which was not so obvious as a result of overlapping with the adsorption of C–C/C-H. Apart from these, the peaks detected at 1651 cm^{-1} (C = O stretching of amide group) and 3363 cm^{-1} (O–H stretching of carboxylic acid) indicated the successful formation of the PA layer. As can be seen, the membrane made with PIP alone as well as those made with the PIP/AEE did not significantly change the PA surface chemistry based on the FTIR spectra shown. The only slight variation in peak noticed was for the membrane made with pure AEE which had a sharp peak at 1649 cm^{-1} corresponding to a C = O stretching of amide group and an enhanced peak at 1488 cm^{-1} which corresponds to N–H bending vibration of amide group of AEE. Similar findings were reported by Perera et al. (2015) and Hosseinzadeh et al. (2018) in which there was no difference or obvious variation in the peaks of fabricated membranes when 1,3–diamino-2-hydroxypropane (DAHP) and monoethanolamine (MEA)/diethanolamine (DEA) were, respectively, used as co-amine monomers in aqueous phase during PA layer synthesis.

Although there is not much change on the PA surface chemistry based on the FTIR spectra, the contact angle data as shown in Fig. 3b can differentiate the fabricated TFC membranes. The water contact angle of TFC membrane made with only PIP and AEE was reported at 32.21° and 45.7°, respectively. As can be seen, by reducing the amount of AEE in the PIP:AEE weight ratio, it resulted in a gradual decrease in the water contact angle from 32.21° to 24.96°. Since PS substrate layer is hydrophobic, introducing a hydrophilic monomer like AEE improves membrane hydrophilicity. Therefore, as AEE weight ratio increases in the membrane PA layer composition, hydrophilicity increases hereby lowering the water contact angle. On the other hand, the membrane cross-linking was not negatively affected upon the introduction of AEE. This will be further discussed in the following section. By comparing to the TFC membrane made of pure PIP (PIP:AEE ratio of 2:0), the contact angle of the best AEE-modified membrane (PIP:AEE ratio of 1.75:0.25) was reduced by ~ 55%, indicating the introduction of small amount of co-amine monomer into PIP aqueous solution could play a significant role in improving membrane surface hydrophilicity. Figure 4 shows the cross-linked PA structure that is developed using different monomer systems.

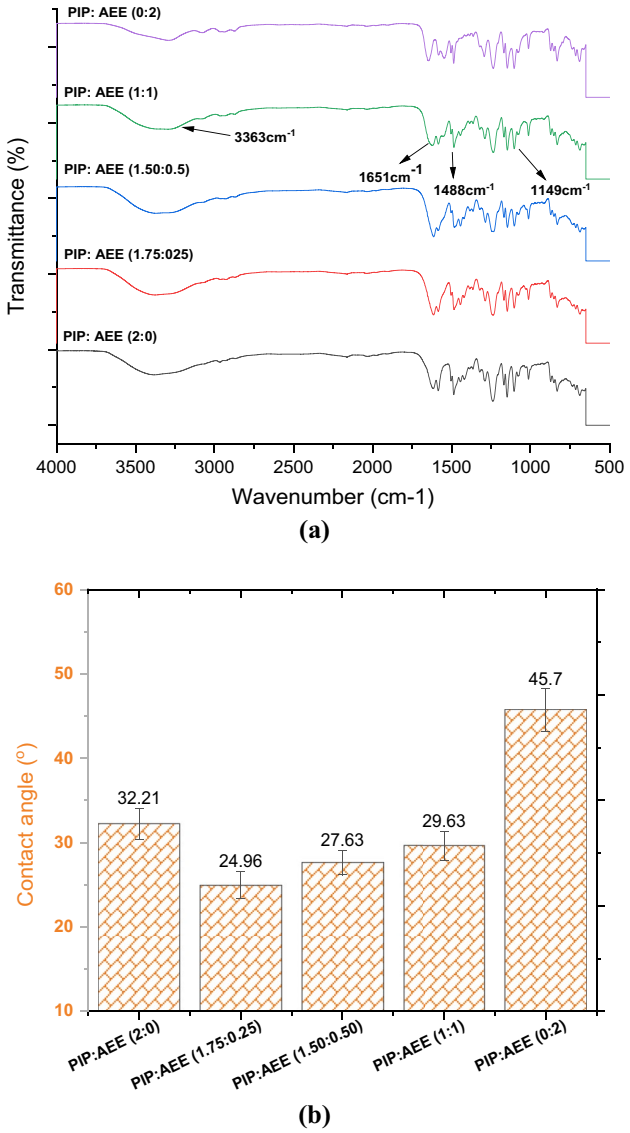

Fig. 3 Properties of TFC membranes made of different PIP:AEE weight ratio, **a** FTIR spectra and **b** water contact angle

TFC membrane morphology

Figure 5 compares the cross section and surface morphologies of TFC membranes made of different PIP: AEE weight ratio in the presence of 0.5 wt% $NaHCO_3$. The detection of nodular structure on the surface of substrate is a clear evidence showing the formation of cross-linked PA selective layer. Figure 5a shows the properties of TFC membrane with PA formed via IP between PIP and TMC. The results were similar to other PIP/TMC membranes as reported in the work of Shen et al. (2020). By comparing this membrane with the membrane made of PIP:AEE ratio of 1:1 (Fig. 5b), it is found that the thickness of the selective layer was increased (to an average of 135 nm) and its surface was relatively rougher with larger nodules. This is attributed to its short molecular chain that limits its diffusion towards TMC in organic phase as well as the stress in the course of the IP process and swelling phenomena during the curing process. AEE monomer dissolved at a slower rate compared to PIP hereby resulting in a smaller granular morphology. A work done by Guo et al. (2020) also indicated this mechanism when N,N-diethylethylenediamine (DEEDA) was introduced into PIP aqueous solution to slow down its diffusion with TMC to develop a cross-linked PA layer with more ridges and rougher surface. For the TFC membrane made of pure AEE (Fig. 5c), its PA selective layer was still thicker compared to the membrane made of pure PIP. In terms of surface morphology, this membrane showed less nodular structure compared to the membrane made of co-amine monomers.

TFC membrane performance

Figure 6 shows the membrane transport properties with respect to water permeability and separation efficiency determined in the NF mode. Generally, the lower the membrane water permeability, the higher its salt rejection and the lower the salt passage. Such relationship is typically reported in the studies related to the TFC NF membrane (Yang et al., 2019). In this work, the water permeability of TFC membrane was reduced from 2.66 L/m^2.h.bar for the PIP:AEE ratio of 2:0 to 1.08 L/m^2.h.bar for the PIP:AEE ratio of 1:1, indicating the presence of more AEE in the PIP aqueous solution could form a denser and/or thicker PA layer that increases the water transport resistance. With respect to separation efficiency, the membrane made of PIP:AEE ratio of 1.50:0.50 and 1:1 showed greater Na_2SO_4 rejection than that of pure PIP membrane, confirming the increase in PA layer thickness (Fig. 5) that created a greater resistance in retaining dissolved ions. The membrane made of pure AEE meanwhile was the best membrane in filtering divalent salt as it achieved the highest Na_2SO_4 rejection (99.5%). Compared to the membrane made of pure PIP, the PA layer of pure AEE membrane was 27% thicker and thus could create greater resistance towards water molecules and dissolved ions, leading to the lowest salt passage as evidenced.

Membrane antifouling performance

Antifouling properties of selected fabricated TFC membranes were evaluated using feed solution composed of 500 ppm BSA and the results are presented in Fig. 7. As can be seen, all the selected membranes experienced flux decline as a function of filtration time and this was due to the depositions/adsorption of foulant on the respective membrane surface that created additional transport resistances for water molecules to pass through. Comparing the three selected membranes, it was found that the water flux of the pure PIP membrane was the highest followed by the PIP/AEE membrane and the pure AEE membrane. Although

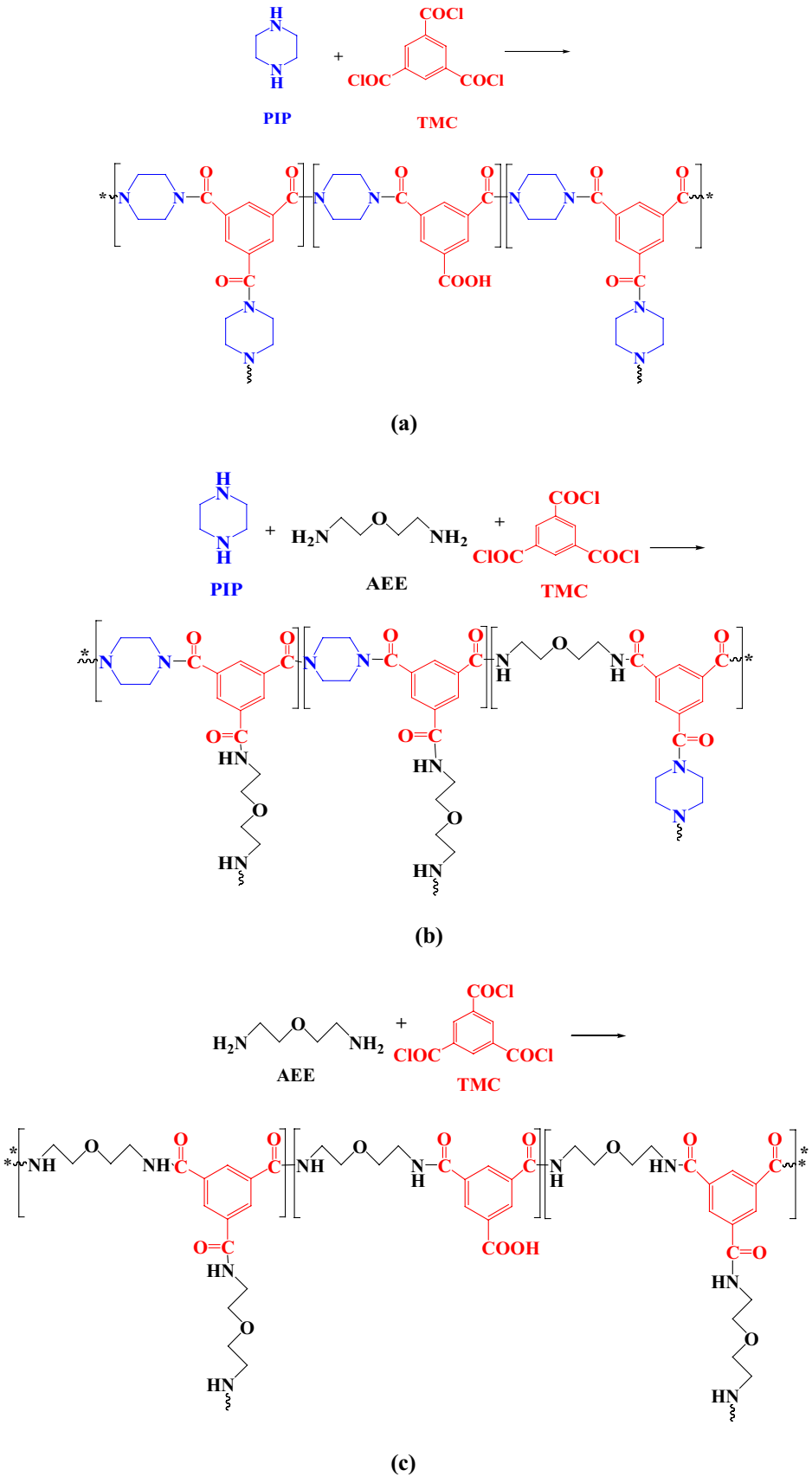

Fig. 4 Structure of different cross-linked PA layer, **a** PIP-TMC, **b** PIP/AEE-TMC and **c** AEE-TMC

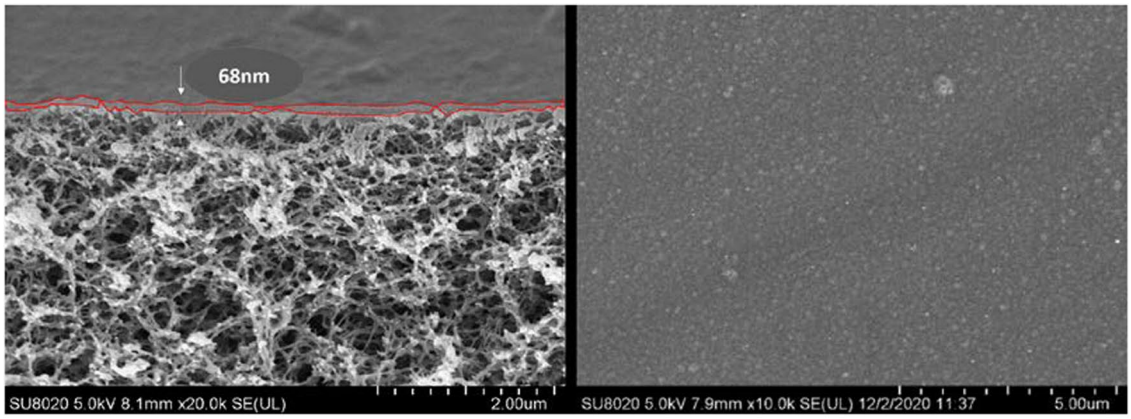

(a)

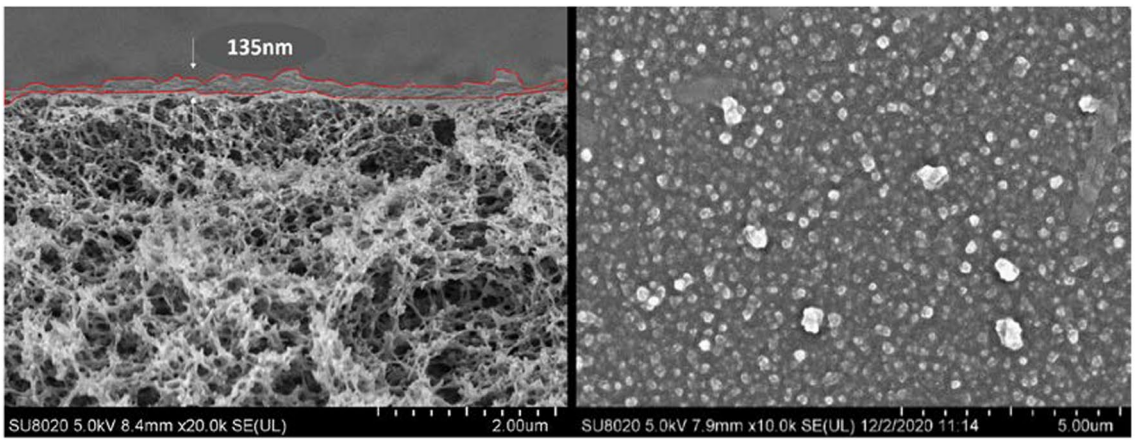

(b)

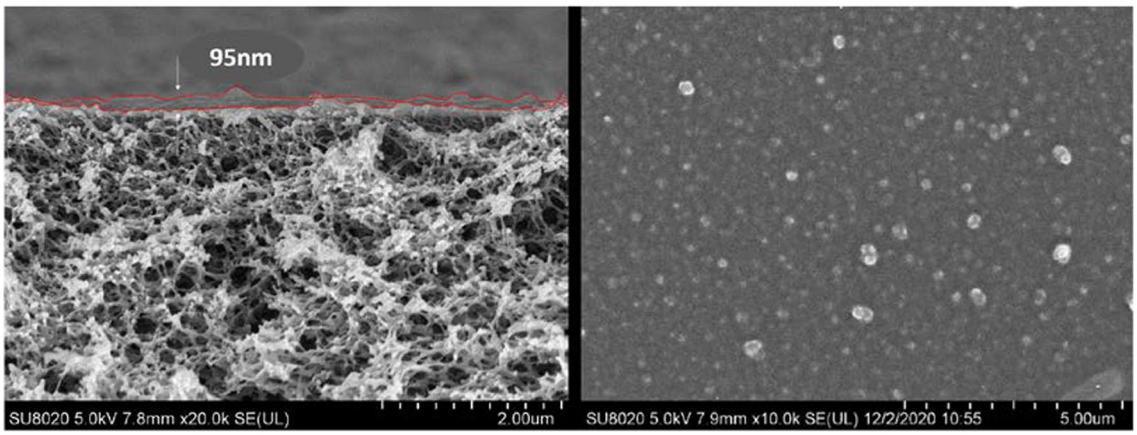

(c)

Fig. 5 FESEM images of cross section (left) and surface morphology (right) of membrane made of different PIP:AEE weight ratio, **a** 2:0, **b** 1:1 and **c** 0:2

both PIP/AEE and pure AEE membranes exhibited lower water permeability, they showed higher degree of FRR, recording 90.2 and 95.7%, respectively. These values were higher than the value achieved by the pure PIP membrane (86.1%).

The higher FRR of the PIP/AEE and pure AEE membranes is simply because of the hydrophilic characteristics of AEE that strengthens its binding to water and reduce foulant adsorption, making the resultant membranes easy to clean. Although the

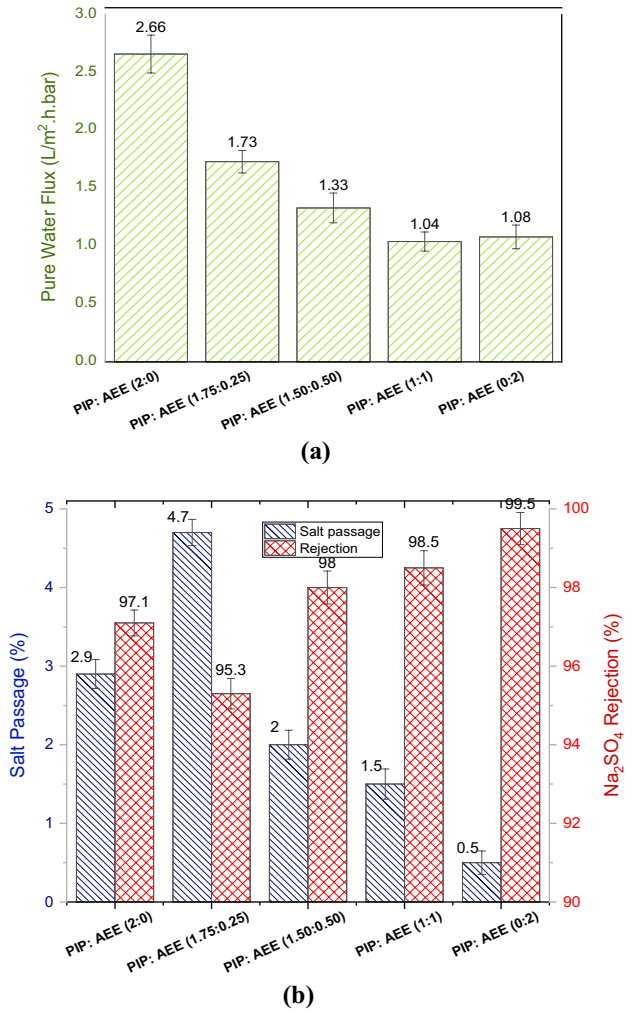

Fig. 6 Effect of PIP:AEE weight ratio on TFC membrane performance with respect to **a** pure water flux and **b** salt passage and Na_2SO_4 rejection

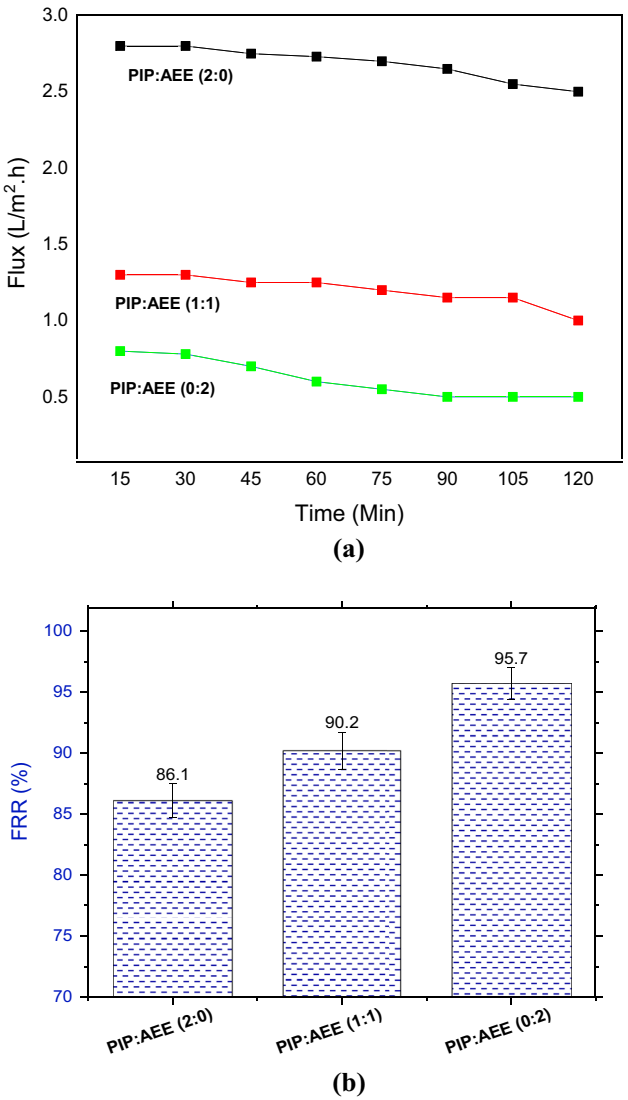

Fig. 7 **a** Flux behaviour of selected TFC membranes subjected to 500-ppm BSA feed solution as a function of filtration time and **b** FRR of the fouled membranes after being cleaned by water

contact angle of the AEE membrane was higher compared to the pure PIP membrane (Fig. 3), such findings cannot be precisely used to indicate the surface hydrophilicity of resultant membrane. This is because the increase in the roughness of pure AEE membrane (Fig. 5) might alter the interaction between water molecules and PA surface, leading to higher contact angle. Previous studies conducted by Ji et al. (2019) and Kazemi et al. (2020) also reported that the use of 3,3-diaminobenzidine and 1,2,4-triaminibenzene as hydrophilic co-amine monomers could enhance antifouling performance of membrane. Their results showed that the modified TFC membranes exhibited a FRR of ~ 95% compared to 85.5% shown by the control membrane after being subjected to several hours of testing.

Performance of membranes for AT-POME treatment

Figure 8a shows the performance of selected TFC membranes for the treatment of AT-POME with respect to several important parameters. Unlike POME, AT-POME contains much lower organic pollutants as it has been aerobically treated on site to significantly reduce the levels of COD and other large molecules (Ng et al. 2020). The characteristics of AT-POME are as follows: Conductivity (μS/cm): 5982 (±23), colour (ADMI): 610 (±17), colour (Abs): 2.82 (±0.03), pH: 8.87 (±0.21) and COD (mg/L): 308 (±0.5).

As it can be seen, all the selected membranes showed very promising results in removing Colour (ADMI) and Colour (Abs), recording at least 92.79% and 91.13% reduction, respectively. In addition, they also exhibited good rejection for the COD, achieving at least 83.4%. All permeates clearly showed an absolutely colourless without any form of particles. Conductivity reductions as shown by these TFC membranes however were slightly lower as the developed membranes are in the NF

category and might not be efficient to remove most of the dissolved ions present in the AT-POME. Without any doubt, all these three membranes showed reasonably good performance in treating AT-POME. Their separation rates were comparable with relevant studies that used commercial TFC membranes (i.e., NF90 and NF270) for AT-POME treatment with colour rejection ranging from 96–97% (Abdullah et al. 2018). However, it must be emphasized that the PIP/AEE and pure AEE membranes in fact demonstrated better separation efficiencies compared to the pure PIP membrane. These findings are correlated to their higher Na_2SO_4 rejection as presented in Fig. 6b.

The FRR of the fouled TFC membranes after being cleaned by pure water (Fig. 8b) indicated that the deposition of more foulants on the pure AEE membrane has significantly reduced its FRR compared to the PIP/AEE and pure PIP membranes, although this membrane was the best performing membranes in separating Na_2SO_4 and impurities from the AT-POME. Further research is still required to further improve the surface-modified TFC membranes for AT-POME treatment.

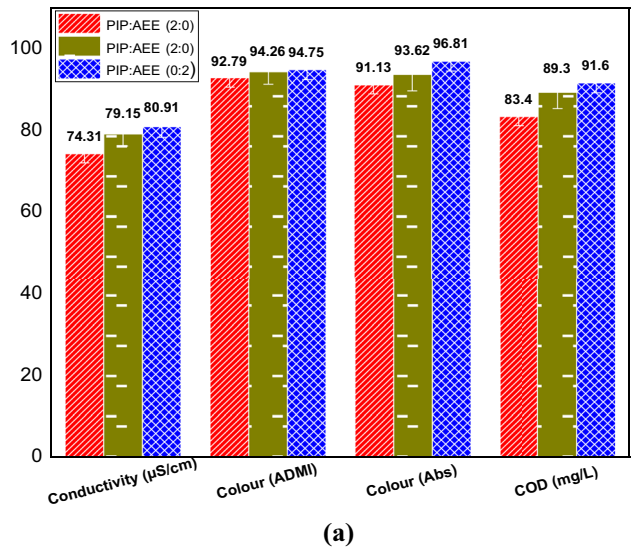

(a)

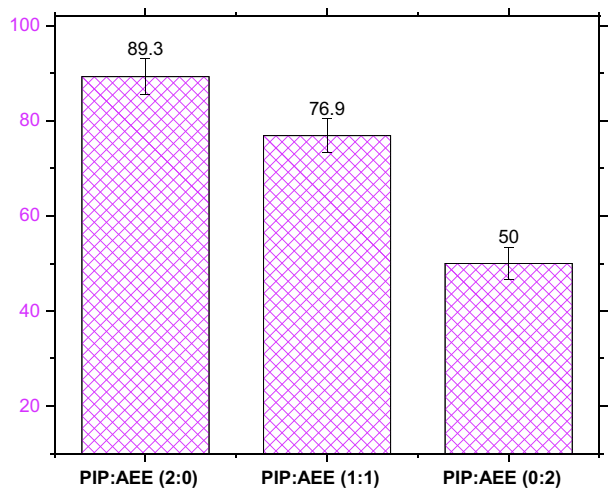

(b)

Fig. 8 **a** Separation performances of different TFC membranes for AT-POME treatment and **b** FRR of different TFC membranes subjected to AT-POME feed solution after being cleaned by water

Conclusion

In this work, different types of PA TFC membranes with various properties were fabricated by varying the loading of $NaHCO_3$ and co-amine monomer weight ratio in the aqueous solution during IP process. The experimental results showed that the introduction of $NaHCO_3$ in the PIP aqueous solution could affect the membrane PA layer surface, making it looser. Membrane hydrophilicity was also gradually increased by increasing $NaHCO_3$ loading from 0.5 to 3.5 wt%, resulting in an increase in water flux from 2.58 to 4.12 L/m^2.h.bar. However, the presence of > 0.5 wt% $NaHCO_3$ in the PIP solution could negatively affect the membrane rejection against Na_2SO_4 and thus should be controlled at 0.5 wt%. By fixing $NaHCO_3$ loading at 0.5 wt%, the impacts of PIP:AEE weight ratio on the properties of TFC membranes were studied and the findings showed that the PA layer became denser and slightly rougher as the weight of AEE monomer was increased. Compared to the PIP-based membrane (control) that showed only 97.1% Na_2SO_4 rejection, the membranes made of PIP:AEE ratio of 1:1 and pure AEE achieved better rejection, i.e., 98.5 and 99.5%, respectively. Further evaluation indicated that the membrane made of PIP:AEE ratio of 1:1 was effective to treat AT-POME by reducing the solution's conductivity, colour (ADMI) and COD by 79.15%, 94.26% and 89.3%, respectively, compared to the PIP-based membrane which only attained lower performance, i.e., 74.31, 92.79 and 83.4%, respectively. Besides demonstrating the potential roles in improving the membrane salt rejection and antifouling properties, the AEE-modified membrane when tested with AT-POME also achieved a better separation performance compared to the typical PIP-based membranes with respect to COD, colour, and conductivity removal. However, the modified membrane showed lower FRR than that of typical PIP-based membrane in the AT-POME treatment. This could be due to its higher separation rate that caused more foulants to deposit on its surface, making the simple pure water rinsing ineffective to recover its water flux. More research is still required to address this issue.

Funding The authors are thankful to Universiti Teknologi Malaysia (UTM) for providing financial support under UTMSHINE Signature Research Grant (Q.J130000.2451.07G79).

Declarations

Conflict of interest The authors declare that they have no known competing financial interests or personal relationships that could have appeared to influence the work reported in this paper.

References

Abdullah WNAS, Lau WJ, Aziz F, Emadzadeh D, Ismail AF (2018) Performance of nanofiltration-like forward-osmosis membranes for aerobically treated palm oil mill effluent. Chem Eng Technol 41(2):303–312. https://doi.org/10.1002/ceat.201700339

Chen F, Peldszus S, Elhadidy AM, Legge RL, Van Dyke MI, Huck PM (2016) Kinetics of natural organic matter (NOM) removal during drinking water biofiltration using different NOM characterization approaches. Water Res 104:361–370. https://doi.org/10.1016/j.watres.2016.08.028

Chong C-J, NorhanizaYusof G-S, FauziIsmail A (2019) Roles of nanomaterial structure and surface coating on thin film nanocomposite membranes for enhanced desalination. Compos B Eng 160:471–479. https://doi.org/10.1016/j.compositesb.2018.12.034

Fan X, Dong Y, Su Y, Zhao X, Li Y, Liu J, Jiang Z (2014) Improved performance of composite nanofiltration membranes by adding calcium chloride in aqueous phase during interfacial polymerization process. J Membr Sci 452:90–96. https://doi.org/10.1016/j.memsci.2013.10.026

Guo YS, Yan-LiJi BinWu, Nai-XinWang M-J, Quan-FuAn C-J (2020) High-flux zwitterionic nanofiltration membrane constructed by in-situ introduction method for monovalent salt/antibiotics separation. J Membr Sci 593:117441. https://doi.org/10.1016/j.memsci.2019.117441

Hao X, Gao S, Tian J, Sun Y, Cui F, Tang CY (2019) Calcium-carboxyl intrabridging during interfacial polymerization: a novel strategy to improve antifouling performance of thin film composite membranes. Environ Sci Technol 53(8):4371–4379. https://doi.org/10.1021/acs.est.8b05690

Hosseinzadeh MT, Hosseinian A (2018) Novel thin film composite nanofiltration membrane using monoethanolamine (MEA) and diethanolamine (DEA) with m-phenylenediamine (MPD). J Polym Environ 26(4):1745–1753. https://doi.org/10.1007/S10924-017-1063-9

Huang BQ, Tang YJ, Zeng ZX, Xu ZL (2020) Microwave heating assistant preparation of high permselectivity polypiperazine-amide nanofiltration membrane during the interfacial polymerization process with low monomer concentration. J Membr Sci 596:117718. https://doi.org/10.1016/j.memsci.2019.117718

Ji Y-L, YapAng MBM, Shu-HsienHuang J-Y, Sheng-JuTsai MR, Guzman De, Hui-AnTsai C-C, La Kueir-RarnLee J-Y (2019) Performance evaluation of nanofiltration polyamide membranes based from 3,3′-diaminobenzidine. Sep Purif Technol 211:170–178. https://doi.org/10.1016/j.seppur.2018.09.067

Jiang Y, Zhang Y, Chen B, Zhu X (2019) Membrane hydrophilicity switching via molecular design and re-construction of the functional additive for enhanced fouling resistance. J Membr Sci 588:117222. https://doi.org/10.1016/j.memsci.2019.117222

Kazemi M, Jahanshahi M, Peyravi M (2020) 1,2,4-Triaminobenzene-crosslinked polyamide thin-film membranes for improved flux/anti-fouling performance. Mater Chem Phys 255:123592. https://doi.org/10.1016/j.matchemphys.2020.123592

Lau WJ, Ismail AF, Misdan N, Kassim MA (2012) A recent progress in thin film composite membrane: a review. Desalination 287:190–199. https://doi.org/10.1016/j.desal.2011.04.004

Li Y, Su Y, Li J, Zhao X, Zhang R, Fan X, Zhu J, Ma Y, Liu Y, Jiang Z (2015) Preparation of thin film composite nanofiltration membrane with improved structural stability through the mediation of polydopamine. J Membr Sci 476:10–19. https://doi.org/10.1016/j.memsci.2014.11.011

Liu M, Chen Q, Lu K, Huang W, Lü Z, Zhou C, Yu S, Gao C (2017) High efficient removal of dyes from aqueous solution through nanofiltration using diethanolamine-modified polyamide thin-film composite membrane. Sep Purif Technol 173:135–143. https://doi.org/10.1016/j.seppur.2016.09.023

Misdan N, Lau WJ, Ismail AF, Matsuura T (2013) Formation of thin film composite nanofiltration membrane: effect of polysulfone substrate characteristics. Desalination 329:9–18. https://doi.org/10.1016/j.desal.2013.08.021

Mollahosseini A, Abdelrasoul A (2019) Recent advances in thin film composites membranes for brackish groundwater treatment with critical focus on Saskatchewan water sources. J Environ Sci 81:181–194. https://doi.org/10.1016/j.jes.2019.01.014

Ng ZC, Chong CY, Sunarya MH, Lau WJ, Liang YY, Fong SY, Ismail AF (2020) Reuse potential of spent RO membrane for NF and UF process. Membr Water Treat 11:323–331. https://doi.org/10.12989/mwt.2020.11.5.323

Noresah S, Khoo YS, Lau WJ, Gürsoy M, Karaman M, Ting TM, Abouzari-Lotf E, Ismail AF (2020) Rapid surface modification of ultrafiltration membranes for enhanced antifouling properties. Membranes 10(12):401. https://doi.org/10.3390/membranes10120401

Origomisan JO, Lau WJ, Aziz F, Ismail AF (2021) Impacts of secondary mixed monomer on properties of thin film composite (TFC) nanofiltration and reverse osmosis membranes: a review. Recent Patents Nanotechnol. https://doi.org/10.2174/1872210514

Pan Y, Xu R, Lü Z, Yu S, Liu M, Gao C (2017) Enhanced both permselectivity and fouling resistance of poly(piperazine-amide) nanofiltration membrane by incorporating sericin as a co-reactant of aqueous phase. J Membr Sci 523:282–290. https://doi.org/10.1016/j.memsci.2016.10.011

Perera DHN, Song Q, Qiblawey H, Sivaniah E (2015) Regulating the aqueous phase monomer balance for flux improvement in polyamide thin film composite membranes. J Membr Sci 487:74–82. https://doi.org/10.1016/j.memsci.2015.03.038

Rezania H, Vatanpour V, Shockravi A, Ehsani M (2019) Study of synergetic effect and comparison of novel sulfonated and carboxylated bulky diamine-diol and piperazine in preparation of negative charge NF membrane. Sep Purif Technol 222:284–296. https://doi.org/10.1016/j.seppur.2019.04.043

Seah MQ, Lau WJ, Goh PS, Tseng H-H, Wahab RA, Ismail AF (2020) Progress of interfacial polymerization techniques for polyamide thin film (Nano)composite membrane fabrication: a comprehensive review. Polymers 12(12):2817. https://doi.org/10.3390/polym12122817

Shafiq MA, AtifIslam SM, Khan NafisaGull, NadirHussain S, Zahid-Butt MT (2018) Cellulaose acetate based thin film nanocomposite reverse osmosis membrane incorporated with TiO2 nanoparticles for improved performance. Carbohyd Polym 186:367–376. https://doi.org/10.1016/j.carbpol.2018.01.070

Shen K, Li P, Zhang T, Wang X (2020) Salt-tuned fabrication of novel polyamide composite nanofiltration membranes with three-dimensional turing structures for effective desalination. J Membr Sci 607:118153. https://doi.org/10.1016/j.memsci.2020.118153

Sun Y, Jin W, Zhang L, Zhang N, Wang B, Jiang B (2018) Sodium bicarbonate as novel additive for fabrication of composite nanofiltration membranes with enhanced permeability. J Appl Polym Sci 135(23):46363. https://doi.org/10.1002/app.46363

Wu F, Liu X, Au C (2016) Effects of DMSO and glycerol additives on the property of polyamide reverse osmosis membrane. Water Sci Technol 74(7):1619–1625. https://doi.org/10.2166/wst.2016.367

Xie Q, Shao W, Zhang S, Hong Z, Wang Q, Zeng B (2017) Enhancing the performance of thin-film nanocomposite nanofiltration membranes using MAH-modified GO nanosheets. RSC Adv 7(86):54898–54910. https://doi.org/10.1039/C7RA11550D

Zi Y, Zhou Yi, Feng Z, Rui X, Zhang T, Zhang Z (2019) A review on reverse osmosis and nanofiltration membranes for water purification. Polymers 11(8):1–22. https://doi.org/10.3390/polym11081252